Phosphoenolpyruvate- and ATP-Dependent Dihydroxyacetone Kinases: Covalent Substrate-Binding and Kinetic Mechanism[†,‡]

Luis F. Garcia-Alles,[§,∥] Christian Siebold,[§,⊥] Therese Lüthi Nyffeler,[#] Karin Flükiger-Brühwiler,[§] Philipp Schneider,[§] Hans-Beat Bürgi,[#] Ulrich Baumann,[§] and Bernhard Erni*[,§]

Department of Chemistry and Biochemistry and Laboratory for Chemical and Mineralogical Crystallography, University of Berne, CH-3012 Berne, Switzerland

Received July 6, 2004; Revised Manuscript Received August 16, 2004

ABSTRACT: Dihydroxyacetone (Dha) kinases are a sequence-conserved family of enzymes, which utilize two different phosphoryldonors, ATP in animals, plants, and some bacteria, and a multiphosphoprotein of the phosphoenolpyruvate carbohydrate phosphotransferase system (PTS) in most bacteria. Here, we compare the PTS-dependent kinase of *Escherichia coli* and the ATP-dependent kinase of *Citrobacter freundii*. They display 30% sequence identity. The binding constants of the *E. coli* kinase for eleven short-chain carbonyl compounds were determined by acetone precipitation of the enzyme−substrate complexes. They are 3.4 μM for Dha, 780 μM for Dha-phosphate (DhaP), 50 μM for D,L-glyceraldehyde (GA), and 90 μM for D,L-glyceraldehyde-3-phosphate. The k_{cat} for Dha of the PTS-dependent kinase is 290 min^{-1}, and that of the ATP-dependent kinase is 1050 min^{-1}. The K_m for Dha of both kinases is <6 μM. The X-ray structures of the enzyme−GA and the enzyme−DhaP complex show that substrates as well as products are bound in hemiaminal linkage to an active-site histidine. Quantum-mechanical calculations offer no indication for activation of the reacting hydroxyl group by the formation of the hemiaminal. However, the formation of the hemiaminal bond allows selection for short-chain carbonyl compounds and discrimination against structurally similar polyols. The Dha kinase remains fully active in the presence of 2 M glycerol, and phosphorylates trace impurities of carbonyl compounds present in glycerol.

Dihydroxyacetone (Dha)[1] kinases convert Dha into the glycolytic intermediate dihydroxyacetonephosphate (DhaP). Free Dha is produced in large quantities by methylotrophic yeast (*1*) growing on methanol. The reaction is catalyzed by Dha synthase, a peroxisomal enzyme that transfers glycolaldehyde from xylulose-5-phosphate to formaldehyde (transketolase) and thereby produces Dha and glyceraldehyde-3-phosphate (GAP). In bacteria, Dha is produced by oxidation of glycerol (*2*) and possibly by aldol cleavage of fructose 6-phosphate (*3*). Dha plays a role in osmoregulation of yeast and algae (*4*). Similar to other short-chain aldoses and ketoses, Dha cannot be stabilized by intramolecular cyclization and therefore is prone to react intermolecularly. Dha reacts with proteins in nonenzymatic Maillard (*5*) type reactions and forms superoxide radicals by autoxidation (*6*). The chemical reactivity toward proteins may be the basis for its use as a tanning agent (*7*−*9*). Despite the apparently limited role of free Dha in metabolic pathways, genes for Dha kinases and other sequence-conserved proteins of an as yet unknown function are found in the genomes of bacteria, plants, and animals including humans. Dha kinases have been shown to detoxify Dha in yeast (*10*). This could indicate that some Dha kinases may be more important for the chemical stress response than for carbon metabolism (*9*).

There exist two forms of Dha kinases, one that utilizes ATP as a phosphate donor and another that uses a phosphoprotein of the bacterial phosphoenolpyruvate:sugar phosphotransferase system (PTS, Figure 1A). The former occurs in eukaryotes and most bacteria, for instance, in the methylotrophic yeast *Hansuela polymorpha* and *Pichia pastoris* (*11*, *12*) and in glycerol-fermenting bacteria (*13*, *14*) and have been purified from *Citrobacter freundii* and *Klebsiella pneumoniae* (*15*−*17*). The PTS-dependent Dha kinase was noticed first as two strongly upregulated protein spots in the proteome of an *Escherichia coli ptsI* mutant,

[†] This research was supported by Grant 3100-063420 from the SWISS National Science Foundation, a grant from the Secretaria de Estado de Educacion y Universidades to L.F.G.A., and the Ciba-Geigy Jubiläumsstiftung.

[‡] Protein Data Bank accession numbers 1UOE and 1UOD (http://www.rcsb.org/).

* To whom correspondence should be addressed: Departement für Chemie und Biochemie, Universität Bern, Freiestrasse 3, CH-3012 Bern, Switzerland. Telephone: ++41 31 631 43 46. Fax: ++41 31 631 48 87. E-mail: bernhard.erni@ibc.unibe.ch.

[§] Department of Chemistry and Biochemistry.

[∥] Present address: Institut de Pharmacologie et de Biologie Structurale, 205, route de Narbonne, F-31077 Toulouse, France.

[⊥] Present address: The Division of Structural Biology and The Oxford Protein Production Facility, The Henry Wellcome Building for Genomic Medicine, Roosevelt Drive, Oxford OX3 7BN, U.K.

[#] Laboratory for Chemical and Mineralogical Crystallography.

[1] Abbreviations: Dha, dihydroxyacetone; DhaP, Dha-phosphate; DhaK, Dha-binding subunit of the *E. coli* Dha kinase; DhaL, small subunit of the *E. coli* Dha kinase; GA, glyceraldehyde; GAP, GA-3-phosphate; Clha, chloro-hydroxyacetone; Prv, pyruvate; PEP, phosphoenolpyruvate; Lac, lactate; G3P, glycerol-3-phosphate; G3PDH, G3P dehydrogenase; Im, imidazole; TIM, triose phosphate isomerase; LDH, lactate dehydrogenase; PK, pyruvate kinase; PTS, PEP: sugar phosphotransferase system; EI, enzyme I of the PTS; HPr, heat stable phosphoryl carrier protein of the PTS; DTT, dithiothreitol.

10.1021/bi048575m CCC: $27.50
Published on Web 09/23/2004

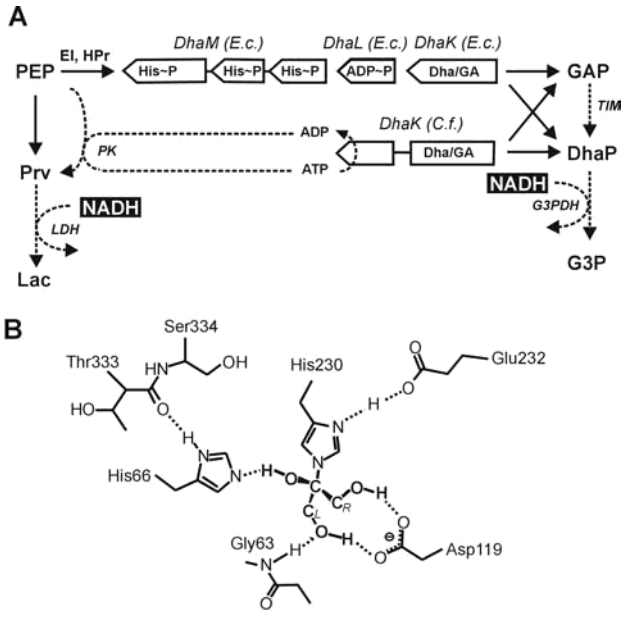

FIGURE 1: Dha kinases. (A) Subunit and domain organization of PTS- and ATP-dependent Dha kinases. The Dha- and nucleotide-binding subunits are indicated. The protein phosphorylation sites are indicated as phosphohistidine and cofactor ADP-P. The enzyme catalyzed reactions used to monitor product formation (Prv, DhaP/GAP) in the coupled assays are indicated by broken arrows. (B) Hemiaminal and hydrogen-bonding interactions between dihydroxyacetone and the *E. coli* DhaK subunit.

which lack enzyme I, the key enzyme of the PTS (*18*). In the ATP-dependent kinase, ATP/ADP exchange is fast. In the PTS-dependent kinase, however, ADP is essentially irreversibly bound to DhaL (DhaL−ADP). Here, ADP serves as a cofactor, which is in situ rephosphorylated by a phosphoprotein of the PTS (Bächler and Erni, to be published elsewhere).

ATP-dependent kinases are two-domain proteins, and PTS-dependent kinases are hetero-oligomeric complexes (Figure 1A). The DhaK subunit/domain consists of two α/β folds (*19*, *20*). Dha is covalently bound in the active site of DhaK through a hemiaminal bond between the C2 of Dha and the Nϵ2 of His-230 (*E. coli*). This chemically labile bond is stabilized by a hydrogen bond between the hemiaminal OH-2 of Dha and the Nϵ2 of His-66, as well as by additional hydrogen bonds between the OH-1 and the OH-3 of Dha and Asp-119 (Figure 1B). The DhaL subunit/domain features an eight-stranded α-helix barrel of regular up−down topology. It contains the nucleotide-binding site at the narrower end of the barrel. The phosphate groups of the nucleotide are coordinated via two magnesium ions to the side-chain carboxyl groups of aspartates. PTS-dependent kinases contain an additional subunit, DhaM. DhaM of *E. coli* consists of three domains, which are homologous to the PTS proteins enzyme I, HPr, and the IIA domain of the PTS transporter for mannose of *E. coli*. The three domains conduct phosphoryl groups from the general phosphorylcarrier protein HPr of the PTS to the DhaL−ADP complex (*21*).

Here, we characterize the substrate specificity and enzyme kinetic properties of the ATP- and PTS-dependent Dha kinases of *C. freundii* (Swiss Prot entry P45510) and *E. coli* (P76015, P76014, and P37349) with different substrates and competitive inhibitors, and we report the X-ray structures of the *E. coli* DhaK subunit in complex with the substrate D-glyceraldehyde (GA) at 2.0 Å resolution and with the product dihydroxyacetone phosphate at 1.9 Å resolution.

EXPERIMENTAL PROCEDURES

Chemicals and Enzymes. Materials were purchased from the following suppliers (in parentheses): pyruvate kinase (PK, 2000 units/mL, Boehringer), L-lactate dehydrogenase (LDH, 2750 units/mL, Boehringer), glycerol-3-phosphate dehydrogenase (G3PDH, 1700 units/mL, Roche), and G3PDH/triose phosphate isomerase mixture (1010 units/mL G3PDH and 9500 units/mL TIM, Fluka), all from rabbit muscle. PEP (cyclohexylammonium salt, Sigma), NADH (disodium salt, Sigma), ATP (disodium salt, Boehringer), dihydroxyacetone (dimer, Fluka), D,L-glyceraldehyde (dimer, Fluka), hydroxyacetone (Fluka), glycerol (>99% pure, Fluka), hydroxypyruvic acid (lithium salt, Fluka), methyl glyoxal (40% aqueous, Sigma), dihydroxyacetone-phosphate (dilithium salt, Fluka), D-erythrose (Fluka), D,L-glyceraldehyde-3-phosphate (Sigma), [2-^{14}C]dihydroxyacetone (50 mCi/mmol, American Radiolabeled Chemicals Inc.).

Synthesis of Chloro-3-hydroxyacetone (Clha). A solution containing 77 mg (0.5 mmol) of 1-acetoxy-3-chloroacetone (TCI America), methanol (0.4 mL), and *tert*-BuOMe (*tert*-butyl-methyl ether, 10 mL) was shaken for 10 min at 37 °C. Lipase B from *Candida antarctica* (0.5 g, Novo Nordisk) was then added. The enzyme was filtered off after 20 min of the reaction; 1 mL of D_2O was added; and most *tert*-BuOMe was evaporated, while taking care not to remove water. The ^{1}H NMR spectrum of the resulting 0.5 M solution was as described (*22*).

Production and Purification of Dha Kinases of E. coli and C. freundii. The DhaK, DhaL, and DhaM subunits of *E. coli* and the Dha kinase of *C. freundii* were purified exactly as described (*20*, *21*).

[^{14}C]Dha Binding Assay. The incubation mixture [100 μL, 5 mg/mL bovine serum albumin, 50 mM NaP_i at pH 7.4, 5 mM $MgCl_2$, 2.5 mM NaF, and 2.5 mM dithiothreitol (DTT)] contained 10 μM DhaK (*E. coli* subunit, *C. freundii* Dha kinase) and between 6 μM and 200 μM [^{14}C]Dha (5750 dpm/nmol). The 100 μL aliquots were incubated for 10 min at room temperature. The enzyme−substrate complex was precipitated with 1 mL of ice-cold 80% acetone, and the protein precipitate was immediately collected on glass microfiber filters (GF/F, Whatman) under suction. The precipitate was washed 3 times with 2 mL of ice cold 80% acetone, and the dried filters were counted in a liquid scintillation counter. K_d was determined by simultaneous nonlinear least-squares fit of P_0 (concentration of covalent Dha−DhaK complex at saturation) and K_d^{Dha} to the data points according to the equation

$$y = 0.5(P_0 + x + K_d^{Dha} - ((P_0 + x + K_d^{Dha})^2 - 4P_0x)^{0.5})$$

with x = [Dha] and y = [^{14}C]Dha−DhaK. Binding of nonradiolabeled substrates was measured in a competition assay at a constant concentration of $L_0 = 100$ μM [^{14}C]Dha (5750 dpm/nmol) and increasing concentrations of the competing substrates. K_i was determined by simultaneous nonlinear least-squares fit of K_i and P_0 (Dha−DhaK concentration at $x = 0$) to the data points according to the equation

$$y = 0.5(P_0 + L_0 + K_d^{Dha}(1 + x/K_i) - ((P_0 + L_0 + K_d^{Dha}(1 + x/K_i))^2 - 4P_0L_0)^{0.5})$$

with x = total concentration of unlabeled substrate, y = [^{14}C]Dha−DhaK complex on the filter, L_0 = 100 μM [^{14}C]Dha, and K_d^{Dha} = 3.4 μM.

Assay for Phosphotransferase Activity. Reactions were performed in 96-well microtiter plates using a Spectramax-250 plate reader as described (*21*). Phosphorylation of Dha or GA was monitored continuously at 30 °C in the presence of G3PDH (final concentration 3 units/mL) or a mixture of G3PDH and TIM (3.5 units/mL G3PDH and 30 units/mL TIM), respectively (Figure 1A). Phosphorylation of substrates other than Dha and GA was monitored by reduction of the pyruvate formed from PEP, which is produced directly by the PTS-dependent Dha kinase and indirectly via an ATP regenerating system by the ATP-dependent kinase (Figure 1A). The reactions were started by addition of the substrate (20 μL) to a preincubated mixture of the complete assay mixture (130 μL) containing 1 mM substrate, 0.7 μM EI, 1 μM HPr, 0.5 μM DhaM, and 0.5 μM DhaL in buffer A (1 mM PEP, 100 mM Hepes buffer at pH 7.5, 5 mM DTT, 5 mM NaF, 5 mM $MgCl_2$, 1 mg/mL BSA, 10 μM EDTA, 7 units/mL LDH, and 0.4 mM NADH). The concentrations of *E. coli* DhaK were varied between 0 and 5.3 μM. The concentration of *C. freundii* DhaK was varied between 0 and 0.82 μM in the presence of 1 mM ATP or 1 mM PEP, 0.1 mM ATPm and 4 units/mL pyruvate kinase.

Inhibition Studies. Phosphorylation of Dha was measured with the G3PDH coupled assay, as indicated above. Half inhibitory concentrations (IC_{50}) were determined by titration of the inhibitor (0−5 mM) in the presence of 0.1 mM Dha and 80−120 nM of DhaK from *E. coli* or 35−260 nM DhaK from *C. freundii*. The reactions were started by addition of 20 μL of a mixture containing 0.75 mM Dha and the inhibitor. K_i values for Clha were determined from the values of K_m^{app} measured for GA (0−1 mM) at four constant concentrations of Clha (0, 33, 100, and 300 μM) after linear regression to the equation $K_m^{app} = K_m(1 + [I]/K_i)$. Enzyme concentrations were 1.7 μM DhaK and 0.5 μM DhaL and DhaM in the *E. coli* system and 0.16 μM DhaK from *C. freundii*. LDH and pyruvate kinase were used as described above.

Crystallization, Structure Solution, and Refinement. Apo-DhaK from *E. coli* was crystallized from 80 mM sodium acetate at pH 5.0, 160 mM $(NH_4)_2SO_4$, 17% (w/v) PEG 4000, and 15% (w/v) MPD using hanging drop vapor diffusion. Crystals of the apo-DhaK were soaked with 2 mM GA or 5 mM DhaP, respectively, and flash-frozen at 105 K. Diffraction data were collected on a RAXIS-IV imaging plate detector mounted on a Rigaku RU300 generator equipped with Yale mirrors (Molecular Structure Corporation, The Woodlands, TX). All data were processed using the HKL program package (*23*). The DhaK structures of complexes were determinded by difference Fourier methods with CNS using the DhaK−Dha complex structure as the template. Refinement was effected using REFMAC (*24*). Details of the crystallographic analysis are shown in Table 3.

Quantum-Mechanical Calculations. Calculations were performed with the Gaussian program package [Gaussian, Inc. (*25*)] using the Density Functional Theory (DFT) at the B3LYP 6-31G** level with a pruned (99 590) grid for integration. Geometries of Dha, imidazole, and the hemiaminal intermediate were optimized with conformations of the heavy atoms, and the hydrogens involved in intermolecular hydrogen bonding were fixed at the values found in the X-ray structure of the DhaK−Dha complex (*19*, *21*). These constraints were necessary to prevent the energy minimization process from ending up in more stable conformations with intramolecular hydrogen bonding (*26*, *27*) unrelated to those found in the crystal structure and therefore of no relevance in the present context. Frequency analysis of imidazole founed an energy minimum. For the tetrahedral intermediate, two imaginary frequencies were found, which involved torsions of terminal hydroxyl groups as expected from fixing their conformations in eclipsed positions. For Dha, three such frequencies appeared, two involving torsions of terminal hydroxyl groups as before, the other one torsions around the C−C bonds. The vibrations corresponding to the three imaginary frequencies tend to deform Dha toward the stable conformation of the isolated molecule with an intramolecular hydrogen bond.

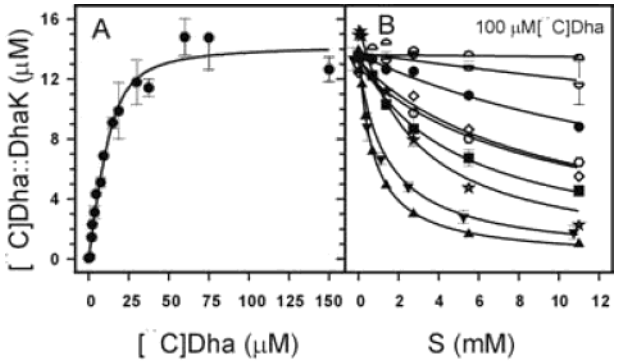

FIGURE 2: Binding of Dha and structural analogues to DhaK. (A) Binding of [^{14}C]Dha to the DhaK subunit of *E. coli*. Average and standard deviation of 5 experiments performed in parallel with experiments shown in B. (B) Displacement of [^{14}C]Dha by the following structural analogues (S) of Dha: D-glyceraldehyde (▲), D,L-glyceraldehyde (▼), D,L-glyceraldehyde-3-phosphate (★), D-erythrose (■), DhaP (●), Cl-Dha (⬡), methyl-glyoxal (◇), hydroxypyruvate (up semicircles), and hydroxyacetone (down semicircles). The total [^{14}C]Dha concentration was 100 μM, and the DhaK concentration was 18 μM.

RESULTS

Substrate Binding and Kinetic Constants. The binding constants of the *E. coli* DhaK subunit for Dha were measured by incubation with increasing concentrations of [^{14}C]Dha and precipitation of the covalent [^{14}C]Dha−DhaK complex with acetone. A representative [^{14}C]Dha binding curve is shown in Figure 2A. The binding constants for unlabeled substrates were measured in competition experiments in the presence of 100 μM [^{14}C]Dha (Figure 2B). The K_d values obtained from these curves are listed in Table 1. The DhaK subunit of *E. coli* has the strongest affinity for Dha (K_d = 3.4 μM) and D-glyceraldehyde (K_d = 25 μM). The (apparent) K_d for racemic D,L-glyceraldehyde is exactly twice (50 μM) indicating that only the D but not the L enantiomer is bound and that binding therefore is enantiospecific. DhaK also binds the product Dha-phosphate (with K_d = 0.8 mM), D-erythrose, methylglyoxal, and Cl-hydroxyacetone but not hydroxypyruvate nor hydroxyacetone (Table 1). The K_d for Dha of the

Table 1: Kinetic Constants of the *E. coli* and *C. freundii* Dha Kinases for Different Substrates

	DhaK/DhaL/DhaM *E. coli*[a]					Dha kinase *C. freundii*[b]				
substrate	K_d (mM)	K_m^{app} (mM)	k_{cat}^{app} (min^{-1})	k_{cat}/K_m (mM^{-1} min^{-1})	IC_{50}[c] (mM)	K_d (mM)	K_m^{app} (mM)	k_{cat}^{app} (min^{-1})	k_{cat}/K_m (mM^{-1} min^{-1})	IC_{50}[c] (mM)
Dha	0.0034	<0.006	290	$>4.9 \times 10^4$		0.07	<0.006	1050	$>1.7 \times 10^5$	
D,L-GA	0.049	0.11	12.5	110	1.7	ND[d]	0.18	310	1.7×10^3	1.1
D-GA	0.025	ND	ND	ND	ND	ND	ND	ND	ND	ND
Clha	0.35	*e*	*e*	<2	1.4	ND	*e*	*e*	<5	≈8[f]
MeGlox[g]	0.34	*e*	*e*	<2	≫5	ND	*e*	*e*	20	≫5
DhaP	0.78	ND	ND	ND	ND	ND	ND	ND	<5	ND
D,L-GAP	0.09	ND	ND	ND	ND	ND	ND	ND	ND	ND
glycerol	>2000	*e*	*e*	<2	≫5	ND	*e*	*e*	<5	≫5
Ha[g]	51	*e*	*e*	<2	≫5	ND	*e*	*e*	45	≫5
HOPyr[g]	2.7	*e*	*e*	<2	≫5	ND	NM[h]	NM	NM	≫5
erythrose	0.18	ND	ND	ND	ND	ND	ND	ND	ND	ND

[a] K_m^{app} and k_{cat}^{app} were determined using the lactate dehydrogenase assay. [b] K_m^{app} and k_{cat}^{app} were determined using the lactate dehydrogenase/pyruvate kinase assay. [c] Determined in the presence of 0.1 mM Dha using the GAP dehydrogenase assay. [d] ND: experiment not done. [e] Below the detection limit of the assay, k_{cat}/K_m are estimated. [f] Extrapolated value. [g] Methylglyoxal, hydroxyacetone, and hydroxypyruvate. [h] NM: not measurable because HOPrv is a substrate of pyruvate kinase.

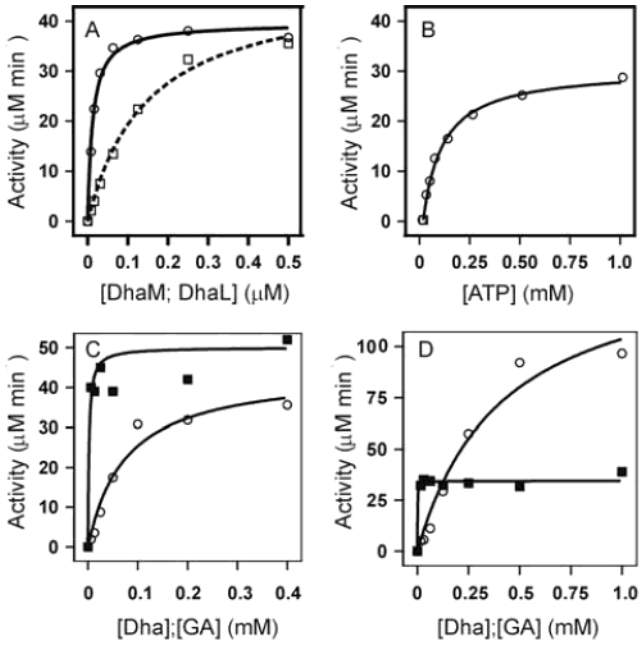

FIGURE 3: Rate of Dha and GA phosphorylation by Dha kinases of *E. coli* (A and C) and *C. freundii* (B and D). (A) Concentration of DhaM (—, ○) and DhaL (- - -, □) subunits was varied. K_m^{app}(DhaM) = 0.012 μM, and K_m^{app}(DhaL) = 0.15 μM. The DhaK subunit was kept constant at 0.3 μM. (B) Concentration ATP (○) was varied K_m^{app}(ATP) = 0.10 mM. DhaK was kept constant at 0.033 μM. (C and D) Concentrations of Dha (■) and GA (○) are varied. (C) DhaK (*E. coli*) concentration was 0.17 μM with Dha (K_m < 5 μM) and 3.7 μM with GA (K_m = 0.11 mM) as the substrate. The DhaL and DhaM concentrations were 0.5 μM. (D) DhaK (*C. freundii*) concentration was 0.033 μM with Dha (K_m < 5 μM) and 0.33 μM with GA (K_m = 0.18 mM). The kinetic constants are listed in Table 1.

C. freundii Dha kinase determined by the same method is between 50 and 70 μM (Table 1).

K_m and k_{cat} of the two Dha kinases for Dha and the phosphoryl donors (phospho-DhaM and ATP) were determined in a coupled assay by enzymatic reduction of DhaP with NADH in the presence of G3PDH (Figure 1). The K_m of the *E. coli* DhaK−DhaL complex for DhaM is 12 nM (Figure 3A), and the K_m of the *C. freundii* DhaK for ATP is 100 μM (Figure 3B). The K_m for Dha is too low for accurate determination because of the limited sensitivity of the assay at small substrate concentrations (small differences of NADH absorbance). The extrapolated K_m values are below 5 μM (solid symbols of parts C and D of Figure 3 and Table 1). The apparent Michaelis constant of DhaK for the DhaL subunit is 0.15 μM (- - -, Figure 3A). The k_{cat} values are 290 min^{-1} for the *E. coli* and 1050 min^{-1} for the *C. freundii* enzyme. These values are of the same order as the kinetic constants previously published for the kinases of *C. freundii*, *Klebsiella*, tomato, and yeast (*15*, *16*, *28*, *29*). GA is a substrate of both the PTS- and ATP-dependent Dha kinases (parts C and D of Figure 3). The K_m of the *E. coli* and *C. freundii* enzymes for D,L-GA are 0.11 and 0.18 mM, with the k_{cat} = 12 and 310 min^{-1}, respectively. The following observations indicate that the reaction is enantiospecific for D-GA (results not shown): (i) enantiomerically pure [^{14}C]-D-GA is phosphorylated quantitatively by the Dha kinase; (ii) only 1 mol of PEP is consumed per 2 mol of D,L-GA; and (iii) the reaction product is tautomerized to DhaP by TIM, which is stereospecific for D-GAP. The latter observation also indicates that GA is phosphorylated at OH-3 and not at OH-2 (see below). GA was used as the substrate in some of the experiments described below because the kinetic constants could be determined more accurately with this substrate.

Competitive Inhibition by Cl-Hydroxyacetone and Substrate Analogues. Several analogues of Dha were tested as inhibitors of the *E. coli* and *C. freundii* Dha kinases. GA and Clha are inhibitors, glycerol, hydroxyacetone, hydroxypyruvic acid, and methylglyoxal are neither substrates nor inhibitors (parts A and B of Figure 4 and Table 1). Clha is of particular interest because it is a haloketone that could react with nucleophilic groups in the active site. According to the ^{1}H NMR spectrum, Clha exists in an aqueous solution as a 1:1 mixture of ketone and ketone hydrate (not shown). Clha is not phosphorylated by Dha kinases, but it inhibits the enzyme of *E. coli* with an IC_{50} of 1.4 mM and the enzyme of *C. freundii* with an IC_{50} of approximately 8 mM at a Dha concentration of 0.1 mM (parts A and B of Figure 4). Additional experiments (parts C and D of Figure 4) show that inhibition of GA phosphorylation is competitive with a K_i of 0.15 and 0.6 mM for the *E. coli* and *C. freundii* kinase, respectively. However, the kinases are not inactivated by incubation with 1 mM Clha for 30 min, by ligand binding

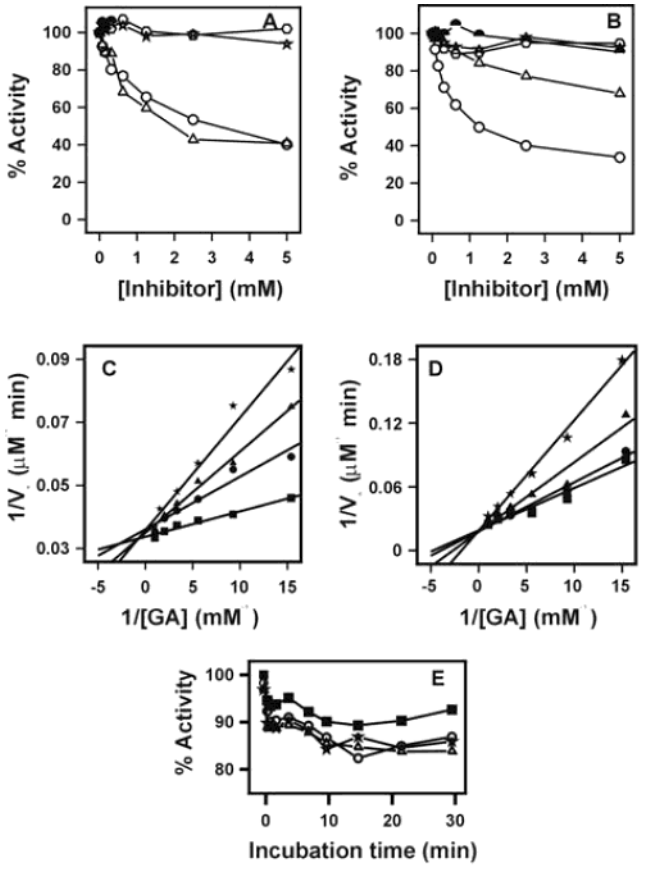

FIGURE 4: Inhibition by Cl-hydroxyacetone and substrate analogues. (A, C, and E) *E. coli* kinase. (B and D) *C. freundii* kinase. (A and B) Inhibition by GA (○), Clha (△), hydroxyacetone, (⬡), glycerol (★), and hydroxypyruvate (semicircles). The IC_{50} constants are listed in Table 1. (C and D) Lineweaver−Burk plots of inhibition by Clha. The Clha concentrations were 0.0, 0.033, 0.1, and 0.3 mM in C and 0.0, 0.1, 0.3, and 0.9 mM (■, ●, ▲, and ★) in D. (E) Reversibility of inhibition by Clha. A total of 35 μM DhaK of *E. coli* was preincubated without (■), with 1 mM Clha alone (○), with 1 mM Clha plus 2.4 μM DhaL (★), and with 1 mM Clha plus complete PTS system under turnover conditions (△). Aliquots were withdrawn at the indicated time points and diluted 20-fold into a standard assay mixture without DhaK. The concentrations were for A, C, and E, 1.7 μM DhaK, 0.5 μM DhaL, and 0.5 μM DhaM plus standard concentrations of EI, HPr, and PEP; and for B and D, 0.17 μM DhaK and 1 mM ATP.

alone, nor under conditions where the bound ligand can react (turnover) (Figure 4E). When taken together, this suggests (i) that Clha is bound to the active site with the Cl group occupying the position of the hydroxyl group of Dha, which is phosphorylated (*pro-R*) and (ii) that the active site does not contain a nucleophilic group strong enough to react with a weak electrophile. The latter conclusion agrees with the X-ray structure, which shows that the entrance to the active-site pocket is free of nucleophilic groups (*19*). The two products, GAP and DhaP, do not inhibit the *C. freundii* Dha kinase at concentrations up to 5 mM (results not shown).

Kinetic Mechanism of Phosphoryl Transfer. Bisubstrate kinetics were measured with the ATP-dependent Dha kinase. The initial rate of GAP formation was determined as a function of the concentrations of GA and ATP at three constant concentrations of ATP and GA, respectively (parts A and B of Figure 5). The values estimated for k_{cat}, K_m, and k_{cat}/K_m obtained from Figure 5 are listed in Table 2. Both k_{cat} and K_m decrease when decreasing concentrations of GA

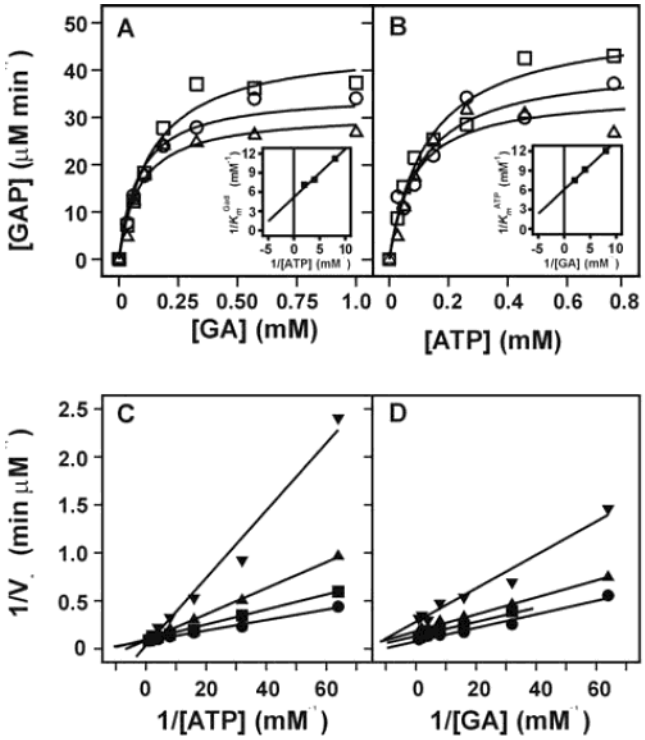

FIGURE 5: Multisubstrate kinetics of the *C. freundii* Dha kinase. (A) Concentration of GA was varied at three concentrations of ATP (0.125, 0.25, and 0.5 mM; △, □, and ○). (B) Concentration of ATP was varied at three concentrations of GA (0.125, 0.25, and 0.5 mM; △, □, and ○). Apparent K_m values for GA and ATP were extracted by nonlinear best fit of the datapoints to the Michaelis−Menten equation. True K_m values were determined by linear regression from the double-reciprocal plots of the apparent K_m for one substrate versus the concentration of the second (insets). (C and D) Inhibition of *C. freundii* kinase by ADP. (A) ADP competes with ATP. (B) ADP inhibits noncompetitively with respect to GA. ADP concentrations were 0.0, 0.033, 0.1, and 0.3 mM (●, ■, ▲, and ▼).

Table 2: Kinetic Constants for the Phosphorylation of D,L-Glyceraldehyde by the Dha Kinases from *C. freundii*

	constant substrate	k_{cat}^{app} (min^{-1})	$K_m^{app\ A,B}$ (μM)	$k_{cat}/K_m^{A,B}$ ($\mu M^{-1}\ min^{-1}$)
Figure 5A[a]	ATP (mM)	Varying GA Concentration (K_m for GA)		
	0.500	280 ± 20	140 ± 30	2.0 ± 0.5
	0.250	238 ± 7	130 ±10	1.9 ± 0.2
	0.125	190 ± 10	90 ± 20	2.1 ± 0.6
	constant substrate	k_{cat}^{app} (min^{-1})	$K_m^{app\ A,B}$ (μM)	$k_{cat}/K_m^{A,B}$ ($\mu M^{-1}\ min^{-1}$)
Figure 5B[a]	GA (mM)	Varying ATP Concentration (K_m for ATP)		
	0.500	300 ± 20	130 ± 40	2.3 ± 0.7
	0.250	250 ± 20	110 ± 30	2.3 ± 0.7
	0.125	210 ± 20	80 ± 30	2.6 ± 0.9

[a] Kinetic constants were extracted from the results shown in Figure 5.

and ATP are used (three constant concentrations), whereas the specificity constants k_{cat}/K_m remain constant at around 2.3 and 2.0 $\mu M^{-1}\ min^{-1}$, respectively. The k_{cat}/K_m for each substrate appears to be independent of the concentration of the second substrate. The real K_m values were obtained from the double-reciprocal plots [insets of Figure 5 (*30*)]. They are 0.12 mM for GA and 0.14 mM for ATP. Constant k_{cat}/K_m (parallel-line reciprocal plots) are the hallmark of ping-pong kinetics, although other kinetic pathways also can give rise to similar outcomes. The X-ray structure of the Dha

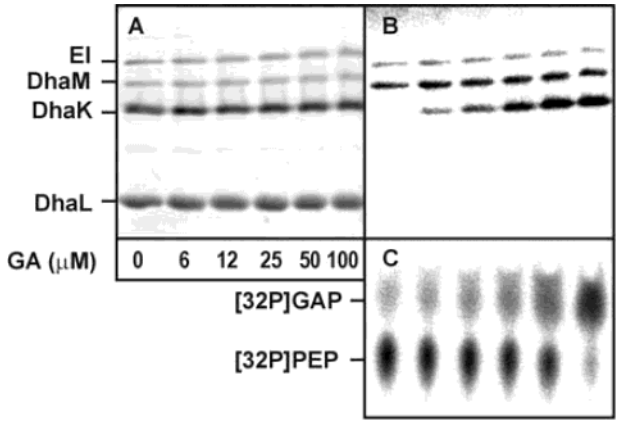

FIGURE 6: Stability of the GAP−DhaK complex. Phosphorylation of GA with [^{32}P]PEP. (A) Coomassie-blue-stained polyacrylamide gel. (B) Autoradiogram of polyacrylamide gel. (C) Section of thin-layer chromatogram. The incubation mixture (30 μL) contained 0.97 μM EI, 1.2 μM HPr, 1.25 μM DhaM, 14.3 μM DhaL, 8.9 μM DhaK, 100 μM [^{32}P]PEP and the indicated concentration of GA, 50 mM NaPi at pH 7.5, and 5 mM $MgCl_2$. After incubation for 5 min at 37 °C, 1 μL was spotted for thin-layer chromatography (polyetyleneimine cellulose, 0.85 M KPi at pH 3.4), while the remaining 29 μL were diluted with gel electrophoresis sample buffer and, without heat denaturation, separated on two 20% polyacrylamide gels. One gel was stained with Coomassie blue (A), and the other was soaked in 5% glycerol Tris-HCl at pH 8.5, dried, and autoradiographed (B).

kinases revealed that the binding sites for ATP and GA are located on different loosely coupled domains pointing to a random bi-bi rather than ping-pong mechanism. Moreover, phosphate exchange between [^{14}C]Dha and [^{12}C]DhaP occurred only in the presence of ADP but not in its absence (results not shown).

Product inhibition experiments were performed to further characterize the reaction mechanism. Inhibition of *C. freundii* Dha kinase by ADP was measured at variable ATP concentrations and either nonsaturating (0.1 mM, Figure 5C) or saturating (1 mM, not shown) GA concentration. In both cases, ADP was competitive with ATP. The estimated value of $K_i = 0.14$ mM at saturating GA is comparable to the $K_m = 0.10$ mM measured for ATP in the same experiment. Inhibition by ADP at variable GA is noncompetitive (mixed type) both at nonsaturating (0.1 mM, Figure 5D) and saturating (1 mM, not shown) concentrations of ATP. These results are consistent with a random bi-bi mechanism and the formation of a dead-end complex enzyme, GA and ADP. They are not consistent with a ping-pong mechanism, where ADP would be a mixed-type inhibitor of ATP and a competitive inhibitor of GA. However, a rapid equilibrium system is also expected to produce intersecting initial velocity patterns with both substrates, ATP and GA. This is not the case for GA, where the lines are close to parallel (Figure 5D). A similar outcome was reported for phosphofructokinase and explained by, in comparison to V_{max}, the much slower rate of substrate release (*31*). Such slow release can be expected in view of the facts that the Dha−kinase complex could be precipitated quantitatively with acetone (see above) and that the product DhaP is covalently bound in the X-ray structure of the DhaK subunit (see below). Although crystals of DhaK in complex with GAP could not be obtained, a DhaK−[^{32}P]GAP complex could be separated by polyacrylamide gel electrophoresis (Figure 6). Unlike EI and DhaM, which are phosphorylated at a histidine independently of whether GA is present or not, DhaK is labeled only in the presence of GA (parts A and B of Figure 6), and [^{32}P]GAP can be identified by thin-layer chromatography (Figure 6C). The resistance to sodium dodecyl sulfate of the DhaK−GAP complex adds evidence for strong binding and slow product release.

Table 3: Statistics of Crystallographic Data and Refinement[a]

Data Collection		
dataset	GA	DhaP
resolution overall (highest bin)	25.0−2.00 (2.10−2.00)	25.0−1.90 (2.00−1.09)
unique reflections	54 971	60 809
redundancy	3.5	3.7
completeness[b]	99.3 (93.7)	94.6 (63.1)
R_{merge} (%)[b,c]	7.4 (23.7)	4.5 (10.0)
$I/\sigma I$[a]	16.1	31.7
Refinement		
dataset	GA	DhaP
resolution range (Å)	25.00−2.00	25.00−1.90
R factor (%)[d]	17.9	16.8
R_{free} (%)[e]	23.0	20.6
rmsd bond lengths (Å)[f]	0.017	0.015
rmsd bond angles (deg)[f]	1.731	1.718
number of reflections	53 425	56 190
residues	684	684
water	486	501
sulfate	2	2
average B factors		
protein	16.2	16.6
waters	28,7	27.5
ligand	20.5	26.6
sulfate	24.7	30.6

[a] PDB accession codes are 1UOE for the complex with glyceraldehydes and 1UOD for the complex with DhaP. [b] Numbers in parentheses are for the high-resolution bin. [c] $R_{merge} = \sum|I - \langle I\rangle|/\sum I$, where I is the intensity of an individual measurement and $\langle I\rangle$ is the average intensity from multiple observations. [d] $R_{factor} = \sum||F_{obs}| - k|F_{calc}||/\sum|F_{obs}|$. [e] R_{free} equals the R factor against 5% of the data removed prior to refinement. [f] rmsd is the root-mean-square deviation from ideal geometry.

X-ray Structure of E. coli DhaK in Complex with GA and DhaP. The *E. coli* DhaK subunit was crystallized as described (*19*), and crystals were soaked in solutions containing racemic D,L-GA, DhaP, and GAP. Two complete data sets were collected to a resolution of 2.0 and 1.9 Å, respectively (Table 3) for complexes with GA and DhaP. Soaking with GAP destroyed the crystals, and cocrystallization also did not afford diffraction-quality crystals. The difference Fourier maps calculated with phases derived from the model of the DhaK−Dha complex (*19*) revealed strong extra positive electron densities into which 1 molecule GA or DhaP, respectively, per monomer could be fitted (Table 3). GA and DhaP are covalently bound as hemiaminal to His-230 and hydrogen bonded to His-66 and Asp-119 (Figure 1B and Figure 7) in a similar way as Dha (*19*). The phosphate at the *pro-R* OH group of the DhaP−His-230 hemiaminal (Figure 7A, PDB accession number 1UOD) is surface-exposed. The hydrogen bond between the *pro-R* OH of the substrate Dha and the γ-carboxyl oxygen of Asp-119 can no longer be formed after esterification with phosphate. As a consequence, the γ-carboxylate group is displaced by a slight rotation of the Cβ−Cγ bond. This loss of one hydrogen bond and the electrostatic repulsion between phosphate and carboxylate might destabilize the enzyme−product complex sufficiently to allow dissociation. Indeed, the in vivo

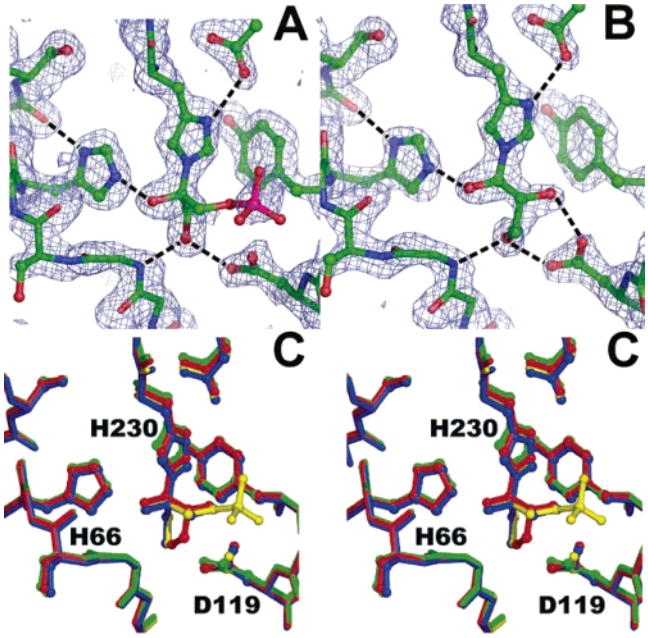

FIGURE 7: Structure of the substrate−active-site complex of the *E. coli* DhaK subunit. (A and B) Experimental $2f_o - f_c$ electron densities of the active site complexed with DhaP and GA at 1.9 and 2.0 Å resolution, respectively, contoured at 1.5 σ. Hydrogen bonds are indicated as black dotted lines. The *pro-R* O−PO_3 of DhaP and the OH-2 of D-GA are on the surface of the active site. (C) Stereoview of the active site with superimposed Dha (blue), DhaP (yellow), D-GA (red), and the apo-DhaK subunit (green).

concentration of DhaP in glycolytically active cells is estimated to be between 0.05 and 0.15 mM (*32*, *33*). Inhibition of Dha kinase activity by DhaP therefore should be insignificant under physiological conditions. The concentration used to soak the crystals was 100 times higher than the physiolgical conditions.

The covalent complex between GA and DhaK is shown in Figure 7B (PDB accession number 1UOE). Bonded is the D isomer, which agrees with the observation that only this isomer is phosphorylated (see above). The OH-3 of GA is hydrogen-bonded to one carboxyl-oxygen atom of Asp-119 and the backbone amide of Gly-63. OH-2 is in hydrogen-bond distance to the carboxyl-oxygen atom of Asp-119. OH-2 of GA is superimposable with the phosphate ester oxygen of DhaP and the *pro-R* OH of Dha (*19*), whereas OH-3 is buried like the *pro-L* OH of DhaP (Figure 7C). One would therefore expect that OH-2 rather than OH-3 is phosphorylated. However, as inferred from the keto-aldol tautomerization of GAP by triosephosphate isomerase (see above), GA must be phosphorylated at OH-3. This and the observation that the k_{cat} for GA is 20-fold smaller and the K_m is 20-fold larger than that for Dha suggest that GA may bind primarily in a nonproductive conformation (*34*).

Biological Function of the Hemiaminal Bond. Catalysis by type-I aldolases proceeds via Schiff base intermediates, formed by condensation of a catalytic lysine with a ketone. The formation of such an intermediate helps to stabilize the development of a negative charge during the aldol cleavage condensation reaction. Whereas hemiaminals of primary amines, such as lysine, can eliminate water to give stable Schiff bases, a hemiaminal with an heteroaromatic system such as imidazole cannot react further and is inherently labile.

What effect, if any, a hemiaminal would exert on the reactivity of a nearby hydroxyl group is not known. Quantum-chemical calculations were performed to estimate whether the carbonyl−hemiaminal transformation affects bond lengths, charge distribution, and basicity of the phosphorylatable OH group of Dha. The geometries of Dha and the Dha imidazole hemiaminal (Dha−Im) were optimized with the constraint of fixing the conformations of heavy atoms and hydrogens involved in intermolecular hydrogen bonds at the values found in the 1.75 Å crystal structure (*19*). Energy-optimization without these geometrical constraints afforded conformations that were unrelated to the X-ray structure and therefore appeared to be of little use. The bond lengths of the phosphorylatable O−H differ by less than 0.0002 Å, and the charges change by less than 0.005 atomic units between Dha and Dha−Im (Table S1 in the Supporting Information). This indicates that the carbonyl−hemiaminal transformation does not affect the nucleophilicity of the α OH group significantly. A similar result is found from a comparison of the protonation energies taken as a measure of the basicity of the α OH groups. The energy of stabilization caused by protonation (C(=O)−C−O($-H_2$)$^+$ versus C(=O)−C−O−H) are −187.5 kcal/mol for the energy-optimized Dha−Im and −184.9 kcal/mol for the energy-optimized Dha. The increased protonation energy in Dha−Im is primarily due to the electrostatic stabilization of the positive charge by the imidazole ring. Provided this effect is not overcompensated by other electrostatic effects in the active site of the protein, it also holds for the positively polarized γ phosphorus atom of ATP and therefore could contribute toward an increased reactivity for phosphorylation. A comparison of the energies of the Dha−Im complex with those of Dha and imidazole shows that the former is more stable than the latter by ∼6 kcal/mol, indicating that the strong affinity of the substrate is due to not only hydrogen bonding in the enzyme−substrate complex but also to covalent bonding. Although this difference is large (Table S1 in the Supporting Information), the conclusions must be taken carefully. Calculations in the gas phase account for the very complex situation in an enzyme only to a limited extent. When these results are taken together, they give no clear-cut indication of an increased reactivity of the α OH group in the hemiaminal, at least not in the ground state.

If the hemiaminal does not control the reactivity of the hydroxyl group, what else could its function be? We tentatively propose that the C−N covalent bond allows the enzyme to discriminate between short-chain carbonyl compounds and the structurally similar polyols. The following experiment illustrates how strong this discrimination can be. After glycerol in a millimolar concentration did not inhibit Dha kinase at all (Table 1), glycerol in molar concentrations was also assayed as a potential substrate. The progress of the kinase reaction was followed spectrophotometrically in a coupled assay with lactate dehydrogenase. As shown in Figure 8A, PEP (NADH) is consumed at a rate of 6.3 μM sec^{-1}. PEP is consumed at the same constant rate at all glycerol concentrations, but the reaction stops earlier when the glycerol concentration is reduced. This behavior suggests that glycerol contains a small amount of a contaminant, which is consumed by the Dha kinase. The ^{32}P-labeled reaction product cochromatographs with [^{14}C]DhaP (Figure 8B). At lower glycerol concentrations, two phases of PEP

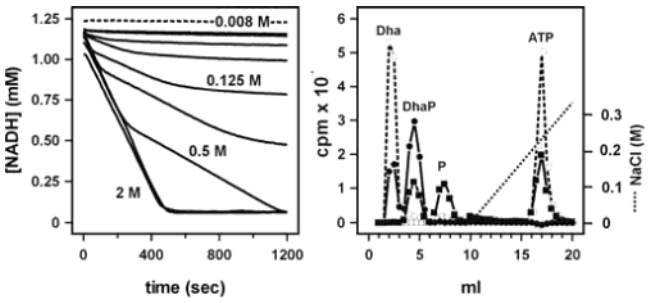

FIGURE 8: Specificity of the *E. coli* Dha kinase for Dha. (A) Reaction with trace amounts of contaminants present in analytical-grade glycerol. *E. coli* Dha kinase was incubated with glycerol (2 M to 8 mM), and the consumption of PEP was followed continuously by reduction of pyruvate with NADH. Two rates are discernible, which might correspond to two substrates. No NADH is consumed when Dha kinase is omitted (- - -). (B) Identification of the phosphorylated product by cochromatography with [^{14}C]Dha. A total of 2.2 M glycerol doped with [^{14}C]Dha was phosphorylated with unlabeled ATP (●), and 2.2 M glycerol (without added Dha) was phosphorylated with [^{32}P]ATP (■). The reaction mixtures were inactivated by heating and then combined and separated on a MonoQ anion-exchange column. The same experiment was repeated without addition of Dha kinase (○ and □). *C. freundii* Dha kinase was used for this experiment.

consumption can be discerned. The fast phase of product formation corresponds to a rate of 380 μM product (μM DhaK^{-1}) min^{-1}, which is comparable to the k_{cat} of Dha kinase for Dha (Table 1). The product corresponding to the slow phase is formed at a rate of 90 μM product (μM DhaK^{-1}) min^{-1}. It could not be isolated by anion-exchange chromatography. According to Figure 8A, >99.5% pure glycerol might contain 0.25% Dha kinase reactive molecules.

DISCUSSION

ATP- and PTS-dependent Dha kinases display a strikingly high degree of sequence and structure similarity. Whereas ATP-dependent kinases have been characterized biochemically and physiologically, little is known of the PTS-dependent kinases. Here, we biochemically characterize the PTS-dependent Dha kinase of *E. coli* and compare it with the ATP-dependent counterpart of *C. freundii*. Dha kinases have a relatively broad substrate specificity for short-chain carbonyl compounds (*28*, *35*, *36*). Dha is the best substrate for both kinases, and GA is second best. X-ray structure and kinetic characterization agree that only the D enantiomer of GA is a substrate, but they disagree with respect to its conformation in the active site. GA is phosphorylated at OH-3, while in the crystalline complex, this group is buried in the binding site. Instead of the primary, the secondary hydroxyl group (OH-2) is surface-exposed and superimposable with the phosphorylatable OH of the Dha complex (Figure 7B). A structure model containing GA in a conformation with the reactive OH-3 at the surface displayed excess electron density and unfavorable stereochemistry for GA (eclipsed bonds, results not shown). It therefore appears that in the crystalline complex GA is bound in the energetically most favorable but nonproductive conformation and that an energetically less favorable conformation with OH-3 at the surface is likely the reactive one. Primary alcohols are more reactive than secondary ones because the former are better solvated (*37*), and this also holds for the enzyme-bound GA in the transition state. In the X-ray structure, enzyme−substrate complementarity may be optimal but enzyme−transition state complementarity might be weak, resulting in high activation energy. For GA bound in a kinetically competent conformation, the situation could then be reversed.

Substrates and products are both covalently bound to the active site by a hemiaminal bond between the carbonyl group and an imidazole nitrogen of a histidine (Figure 7). This covalent binding may give rise to the slow release of the substrate and the observed steady-state kinetics. We propose that this covalent bond determines the specificity of the enzyme for short-chain carbonyl compounds but does not increase the reactivity of the adjacent hydroxyl groups. The reasons for this proposition are 2-fold. First, primary hydroxyl groups in the α (Dha), β (GA), or γ (erythrose) position relative to the carbonyl group are phosphorylated (*28*, *35*, *36*). Second, the quantum mechanically calculated charge distribution, bond length, and bond energy of the phosphorylatable hydroxyl group do not differ significantly between free Dha and Dha in hemiaminal linkage with imidazole. This high selectivity of Dha kinases is in stark contrast to the glycerol kinase, an enzyme of completely different structure (*38*) which does not strongly discriminate between glycerol and Dha (*16*, *39*).

The two kinases have similar substrate specificities and enzyme kinetic constants. The ATP-dependent kinase has a 3 times larger k_{cat} for Dha and a 30-fold larger k_{cat} for GA than the PTS-dependent form. Where both occur concomitantly, as in *Klebsiella pneumoniae* (*40*) and probably also in *C. freundii*, the ATP-dependent form might function as a metabolic enzyme, while the PTS-dependent might act as a sensor for Dha and other short-chain carbonyl compounds. In *E. coli*, which only has a PTS-dependent enzyme, the DhaL and DhaK subunits also function as a coactivator and corepressor of DhaR, the transcription activator of the *dha KLM* operon (Bächler and Erni, to be published elsewhere). The metabolic form may have a higher turnover but low affinity as expected of a catalytic workhorse, while the regulatory form may have a higher affinity but a slower turnover, sufficient to remove the ligand from the binding site and trigger the signaling mechanism.

ACKNOWLEDGMENT

The *C. freundii* genomic DNA was a generous gift from Dr. Rolf Daniel (University of Göttingen). We thank Prof. Irwin H. Segel (University of California—Davis) for his kind advice and stimulating discussions concerning the kinetic part of the present paper.

SUPPORTING INFORMATION AVAILABLE

Table S1, Cartesian coordinates (Å), energies, and thermochemical analysis for all of the optimized structures. This material is available free of charge via the Internet at http://pubs.acs.org.

REFERENCES

1. Waites, M. J., and Quayle, J. R. (1981) The interrelation transketolase and dihydroxyacetone synthase activities in the methylotrophic yeast *Candida boidinii*, *J. Gen. Microbiol. 124*, 309−316.
2. Forage, R. G., and Lin, E. C. (1982) DHA system mediating aerobic and anaerobic dissimilation of glycerol in *Klebsiella pneumoniae* NCIB 418, *J. Bacteriol. 151*, 591−599.

3. Schurmann, M., and Sprenger, G. A. (2001) Fructose-6-phosphate aldolase is a novel class I aldolase from *Escherichia coli* and is related to a novel group of bacterial transaldolases, *J. Biol. Chem. 276*, 11055−11061.
4. Akhtar, N., Blomberg, A., and Adler, L. (1997) Osmoregulation and protein expression in a pbs2δ mutant of *Saccharomyces cerevisiae* during adaptation to hypersaline stress, *FEBS Lett. 403*, 173−180.
5. Tessier, F. J., Monnier, V. M., Sayre, L. A., and Kornfield, J. A. (2002) Triosidines: Novel maillard reaction products and crosslinks from the reaction of triose sugars with lysine and arginine residues, *Biochem. J. 369*, 705−719.
6. Benov, L., and Beema, A. F. (2003) Superoxide-dependence of the short chain sugars-induced mutagenesis, *Free Radical Biol. Med. 34*, 429−433.
7. Draelos, Z. D. (2002) Self-tanning lotions: Are they a healthy way to achieve a tan? *Am. J. Clin. Dermatol. 3*, 317−318.
8. Levy, S. B. (1992) Dihydroxyacetone-containing sunless or self-tanning lotions, *J. Am. Acad. Dermatol. 27*, 989−993.
9. Petersen, A. B., Wulf, H. C., Gniadecki, R., and Gajkowska, B. (2004) Dihydroxyacetone, the active browning ingredient in sunless tanning lotions, induces DNA damage, cell-cycle block, and apoptosis in cultured HaCaT keratinocytes, *Mutat. Res. 560*, 173−186.
10. Molin, M., Norbeck, J., and Blomberg, A. (2003) Dihydroxyacetone kinases in *Saccharomyces cerevisiae* are involved in detoxification of dihydroxyacetone, *J. Biol. Chem. 278*, 1415−1423.
11. Luers, G. H., Advani, R., Wenzel, T., and Subramani, S. (1998) The *Pichia pastoris* dihydroxyacetone kinase is a PTS1-containing, but cytosolic, protein that is essential for growth on methanol, *Yeast 14*, 759−771.
12. van der Klei, I. J., van der Heide, M., Baerends, R. J., Rechinger, K. B., Nicolay, K., Kiel, J. A., and Veenhuis, M. (1998) The Hansenula polymorpha per6 mutant is affected in two adjacent genes which encode dihydroxyacetone kinase and a novel protein, Pak1p, involved in peroxisome integrity, *Curr. Genet. 34*, 1−11.
13. Forage, R. G., and Foster, M. A. (1982) Glycerol fermentation in *Klebsiella pneumoniae*: Functions of the coenzyme B_{12}-dependent glycerol and diol dehydratases, *J. Bacteriol. 149*, 413−419.
14. Ruch, F. E., Lengeler, J., and Lin, E. C. (1974) Regulation of glycerol catabolism in *Klebsiella aerogenes*, *J. Bacteriol. 119*, 50−56.
15. Daniel, R., Stuertz, K., and Gottschalk, G. (1995) Biochemical and molecular characterization of the oxidative branch of glycerol utilization by *Citrobacter freundii*, *J. Bacteriol. 177*, 4392−4401.
16. Johnson, E. A., Burke, S. K., Forage, R. G., and Lin, E. C. (1984) Purification and properties of dihydroxyacetone kinase from *Klebsiella pneumoniae*, *J. Bacteriol. 160*, 55−60.
17. Tong, I. T., Liao, H. H., and Cameron, D. C. (1991) 1,3-Propanediol production by *Escherichia coli* expressing genes from the *Klebsiella pneumoniae* Dha regulon, *Appl. Environ. Microbiol. 57*, 3541−3546.
18. Beutler, R., Kämpfer, U., Schaller, J., and Erni, B. (2001) Heterodimeric dihydroxyacetone kinase from a *ptsI* mutant of *Escherichia coli*, *Microbiology 147*, 249−250.
19. Siebold, C., Garcia-Alles, L. F., Erni, B., and Baumann, U. (2003) A novel mechanism of covalent substrate binding in the X-ray structure of the DhaK subunit of the *Escherichia coli* dihydroxyacetone kinase, *Proc. Natl. Acad. Sci. U.S.A. 100*, 8188−8192.
20. Siebold, C., Arnold, I., Garcia-Alles, L. F., Baumann, U., and Erni, B. (2003) Crystal structure of the *Citrobacter freundii* dihydroxyacetone kinase reveals an eight-stranded-helical barrel ATP-binding domain, *J. Biol. Chem. 278*, 48236−48244.
21. Gutknecht, R., Beutler, R., Garcia Alles, L. F., Baumann, U., and Erni, B. (2001) The dihydroxyacetone kinase of *Escherichia coli* utilizes a phosphoprotein instead of ATP as phosphoryldonor, *EMBO J. 20*, 2480−2486.
22. Chari, R. V. J., and Kozarich, J. W. (1982) Synthesis and properties of halohydroxyacetones and halomethylglyoxals, *J. Org. Chem. 47*, 2355−2358.
23. Otwinowski, Z., and Minor, W. (1997) Processing of X-ray diffraction data collected in oscillation mode, *Methods Enzymol. 276*, 307−326.
24. Murshudov, G. N., Vagin, A. A., Lebedev, A., Wilson, K. S., and Dodson, E. J. (1999) Efficient anisotropic refinement of macromolecular structures using FFT, *Acta Crystallogr., Sect. D 55*, 247−255.
25. Frisch, M. J., Trucks, G. W., Schlegel, H. B., Scuseria, G. E., Robb, M. A., Cheeseman, J. R., Zakrzewski, V. G., Montgomery, J. A., Stratmann, R. E., Burant, J. C., Dapprich, S., Millam, J. M., Strain, M. C. Farkas O., Tomasi, J., Barone, V., Cossi, M., Cammi, R., Mennucci, B., Pomelli, C., Adamo, C., Clifford, S., Ochterski, J., Petersson, G. A., Ayala, P. Y., Cui, Q., Morokuma, K., Malick, D. K., Rabuck, A. D., Raghavachari, K., Foresman, J. B., Cioslowski, J., Ortiz, J. V., Baboul, A. G., Stefanov, B. B., Liu, G., Liashenko, A., Piskorz, P., Komaromi, I., Gomperts, R., Martin, R. L., Fox, D. J., Keith, T., Al-Laham, M. A., Peng, C. Y., Nanayakkara, A., Challacombe, M., Gill, P. M. W., Johnson, B., Chen, W., Wong, M. W., Andres, J. L., Gonzalez, C., Head-Gordon, M., Replogle, E. S., and Pople, J. A. *Gaussian 98* (1998) Revision A.9, Gaussian, Inc., Pittsburgh, PA.
26. Lozynski, M., Rusinska-Roszak, D., and Mack, H.-G. (1997) MP2 and density functional studies of hydrogen bonding in model trioses: D-(+)-Glyceraldehyde and dihydroxyacetone, *J. Phys. Chem. A 101*, 1542−1548.
27. Signorell, R., and Luckhaus, D. (2002) Aerosol spectroscopy of dihydroxyacetone: Gas phase and nanoparticles, *J. Phys. Chem. A 106*, 4855−4867.
28. Herz, S., Kis, K., Bacher, A., and Rohdich, F. (2002) A tomato enzyme catalyzing the phosphorylation of 3,4-dihydroxy-2-butanone, *Phytochemistry 60*, 3−11.
29. Itoh, N., Tujibata, Y., and Liu, J. Q. (1999) Cloning and overexpression in *Escherichia coli* of the gene encoding dihydroxyacetone kinase isoenzyme I from *Schizosaccharomyces pombe*, and its application to dihydroxyacetone phosphate production, *Appl. Microbiol. Biotechnol. 51*, 193−200.
30. Segel, I. H. (1993) *Enzyme Kinetics*, pp 607−612, John Wiley and Sons, Inc., New York.
31. Bar-Tana, J., and Cleland, W. W. (1974) Rabbit muscle phosphofructokinase. II. Product and dead end inhibition, *J. Biol. Chem. 249*, 1271−1276.
32. Fersht, A. (1999) *Structure and Mechanism in Protein Science: A Guide to Enzyme Catalysis and Protein Folding*, W. H. Freeman and Company, New York.
33. Stryer, L. (1988) *Biochemistry*, W. H. Freeman and Company, New York.
34. Jencks, W. P. (1969) *Catalysis in Chemistry and Enzymology*, pp 291−293, McGraw−Hill, Inc., New York.
35. Hofmann, K. H., and Babel, W. (1981) Dihydroxyacetone kinase of methanol-assimilating yeasts. II. Partial purification and some properties of dihydroxyacetone kinase from *Candida methylica*, *Z. Allg. Mikrobiol. 21*, 219−224.
36. Hofmann, K. H., and Babel, W. (1990) Glycerone kinase from *Candida methylica*, *Methods Enzymol. 188*, 451−455.
37. Chaudhary, S. K., and Hernandez, O. (1979) A simplified procedure for the preparation of triphenylmethyl ethers, *Tetrahedron Lett.* 95−98.
38. Hurley, J. H., Faber, H. R., Worthylake, D., Meadow, N. D., Roseman, S., Pettigrew, D. W., and Remington, S. J. (1993) Structure of the regulatory complex of *Escherichia coli* III(Glc) with glycerol kinase, *Science 259*, 673−677.
39. Jin, R. Z., Forage, R. G., and Lin, E. C. (1982) Glycerol kinase as a substitute for dihydroxyacetone kinase in a mutant of *Klebsiella pneumoniae*, *J. Bacteriol. 152*, 1303−1307.
40. Sun, J., Van Den, H. J., Soucaille, P., Qu, Y., and Zeng, A. P. (2003) Comparative genomic analysis of Dha regulon and related genes for anaerobic glycerol metabolism in bacteria, *Biotechnol. Prog. 19*, 263−272.

BI048575M